

A new control structure for PID load frequency control.

Sujit S. Kulkarni¹, Ravindrakumar M. Nagarale²

¹(PG Student, M.B.E.Society's College of, Engineering, Ambajogai (M.S), India)

²(PG Department, M.B.E.Society's College of, Engineering, Ambajogai (M.S), India)

Abstract: This paper deals with load frequency control of power system using new control structure with PID controller. The PID controller is designed for single area and multi area power system. The relay feedback method is used for power system model identification. The PID controller parameters are tuned by expanding controller dynamics using Laurent series. The simulation results shows that the proposed control structure gives better disturbance rejection and robust against uncertainties in plant parameters.

Keywords: Load Frequency Control (LFC), Area Control Error (ACE), Robustness, Relay feedback identification, Laurent series etc.

I. Introduction:

A large-scale power system is composed of multiple control areas that are connected with each other through tie lines [1]. As active power load changes, the frequencies of the areas and tie-line power exchange will deviate from their scheduled values accordingly. As a result, the performance of the power system devices like AC motor, power transformer could be greatly degraded [2]. For example, when frequency is not at its scheduled value then it affects the performance of AC motor, whose speed is depends on supply frequency. Similarly under frequency operation of the power transformer results in low efficiency and over-heating of the transformer windings. To overcome this problem, control of frequency to its scheduled value is an important task in power system. A local governor of the power system can partially compensate power load change through adjusting generator's output. However, with this type of governor, when the system load increases, the system frequency decreases and vice versa [3]. Therefore, a supplementary controller is essential for the power system to maintain the system frequency at 50 Hz (a scheduled frequency in India) no matter what the load is. This type of supplementary controller is called automatic generation control (AGC), or more specifically, load frequency control (LFC). For stable operation of power systems, both constant frequency and constant tie-line power exchange should be provided [4]. Therefore an Area Control Error (ACE), which is defined as a linear combination of power net-interchange and frequency deviations [1], is generally taken as the controlled output of LFC. As the ACE is driven to zero by the LFC, both frequency and tie-line power errors will be forced to zeros as well [1].

In the past six decades, there has been a significant amount of research conducted on LFCs. During the early stage of the research, LFC was based on centralized control strategy [5,6], in which exchange of information takes place from control areas spread over distantly connected geographical territories along with their increased computational problem and storage complexity. In order to overcome the computational limitation, decentralized LFC has recently been developed, through which, each area executes its control based on locally available state variables [7]. Among various types of decentralized LFCs, the most widely employed in power industry is PID control [8–13]. The PI controller tuned through genetic algorithm linear matrix inequalities (GALMIs) [11] becomes increasingly popular in recent years. The PID controller introduced in [13] shows good performance in reducing frequency deviations. However, the robustness of the PID controller for multiple-area power system is not investigated in [13].

In this paper, a new design method for the PID load frequency control is proposed, which considers uncertainties in power system. Even though many advanced control theories have been established, most industrial controllers still use PI or PID. PID controllers are preferred due to easy implementation on analog and digital platform, robustness, wide range applicability and simple structures. Relay feedback identification method is used here for modeling of power system dynamics. PID controller then designed for that identified models. In this Laurent series has been used for tuning of PID controller. The proposed scheme is robust and gives improved performance for disturbance rejection. Simulation examples are provided to show the superiority of the proposed design method.

For clear interpretation, the proposed control structure is presented in section 2. The modeling of single area power system dynamics is given in section 3. Design of controller is addressed in section 4. The multi-area power system is addressed in section 5. Simulation results are presented in section 6 followed by the conclusions in section 7.

II. Proposed control structure:

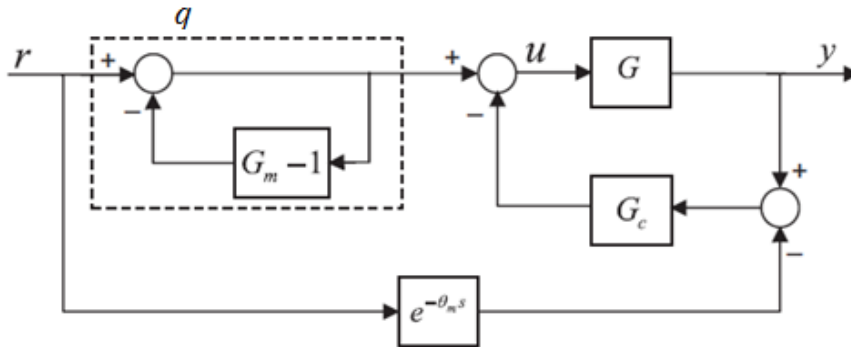


Fig.1. Proposed control structure.

The proposed control structure for LFC is shown in fig.1. in which G_c is PID controller. Unlike the conventional LFC control structure, the proposed structure uses the controller G_c in the feedback path. G_c is used for load disturbance rejection. It also stabilizes the oscillatory process in the loop. G represents the transfer function of overall plant. G_m is the transfer function of the delay free part and θ_m is the time delay part of the plant model. The closed loop transfer function relating the output y to the reference r can be written as:

$$\frac{y}{r} = \frac{G+GG_cG_m e^{-\theta_m s}}{G_m(1+GG_c)} \tag{1}$$

When the plant dynamics and model used exactly matches, equation (1) reduces to:

$$\frac{y}{r} = e^{-\theta_m s} \tag{2}$$

This indicates the system output can reach the set point value just after the process time delay. The block q primarily helps in improving the overall servo performance of the closed loop system. For LFC design it is popularly known that, the load disturbance rejection is more important than the set point response [14]. Therefore, the controller G_c has been designed mainly for power system load disturbance.

III. Single area power system:

Droop Characteristic

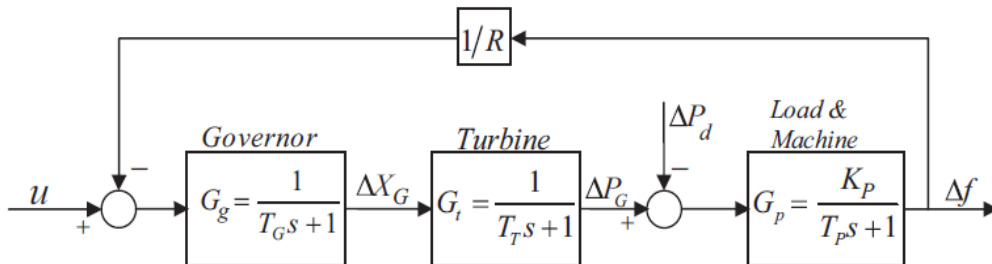


Fig.2. Linear model of single area power system.

In the present work, non- reheat turbine (NRT) and reheat turbine (RT) are considered for LFC modeling. A linear model of a single area power system is shown in fig.2. In which a single generator is supplying power to a single area. In that model G_g , G_t and G_p are the dynamics of the governor, turbine and load & machine, respectively. Non-reheat turbines are first-order units. The dynamics of the non-reheat turbine is represented as $G_t = 1 / (T_t s + 1)$. Reheat turbines are modeled as second-order units, since they have different stages due to high and low steam pressure. The transfer function of the reheat turbine is in the form of $G_t = (cT_r s + 1) / (T_r s + 1)(T_t s + 1)$ where T_r stands for the low pressure reheat time and c is the portion of the power generated by the reheat turbine in the total generated power. The governor dynamics $G_g = 1 / (T_g s + 1)$ and the Load and machine dynamics, $G_p = K_p / (T_p s + 1)$. The plant model used for LFC without droop characteristics is:

$$G = G_g G_t G_p \tag{3}$$

The plant Model Used for LFC with droop characteristic is:

$$G = \frac{G_g G_t G_p}{1 + \frac{G_g G_t G_p}{R}} \tag{4}$$

For LFC, plant model G generally results in higher order, which may be inconvenient for controller design. There are many process identification techniques suggested by various researchers [16–18]. Majhi [19]

introduces a relay based identification method for reducing a higher order process dynamics to a low order dynamics with time delay. This technique has applied here to design a new PID load frequency controller for single-area and multi-area power system. Therefore, these higher order models are approximated by lower order transfer functions with time delay. Equations (3) and (4) can be represented by the second order transfer function model:

$$G = \frac{ke^{-\theta_m s}}{(T_1 s + 1)(T_2 s + 1)} \tag{5}$$

Its state space equation in the Jordan canonical form become:

$$\dot{x}(t) = Ax(t) + bu(t - \theta_m) \tag{6}$$

$$y(t) = cx(t) \tag{7}$$

Where

$$A = \begin{bmatrix} \frac{-1}{T_1} & 0 \\ 0 & \frac{-1}{T_2} \end{bmatrix}, \quad b = \begin{bmatrix} 1 \\ 1 \end{bmatrix}, \quad c = \frac{k}{T_1 - T_2} [1 \quad -1]$$

When a relay test is performed with a symmetrical relay of height $\pm h$, then the expression for the limit cycle output for $0 \leq t \leq \theta_m$ is:

$$y(t) = ce^{At}x(0) + cA^{-1}(e^{At} - I)bh \tag{8}$$

Let the half period of the limit cycle output be τ . Then the expression for the limit cycle output for $\theta_m \leq t \leq \tau$ is:

$$y(t) = ce^{A(t-\theta_m)}x(\theta_m) - cA^{-1}(e^{A(t-\theta_m)} - I)bh \tag{9}$$

The condition for a limit cycle output can be written as:

$$y(0) = cx(0) = -y(\tau) = 0 \tag{10}$$

Substitution of $t = \tau$ in (9) and use of (8) gives the initial value of the cycling states

$$x(0) = (I + e^{A\tau})A^{-1}(2e^{A(\tau-\theta_m)} - e^{A\tau} - I)bh \tag{11}$$

When t_p is the time instant at which the positive peak output occurs and $t_p \geq \theta_m$, then the expression of the peak output A_p becomes:

$$A_p = c(e^{A(t_p-\theta_m)}x(\theta_m) - A^{-1}(e^{A(t_p-\theta_m)} - I)bh) \tag{12}$$

and the expression for the peak time becomes:

$$t_p = \theta_m + \frac{T_1 T_2}{T_1 - T_2} \ln \left(\frac{1 + e^{\frac{-\tau}{T_1}}}{1 + e^{\frac{-\tau}{T_2}}} \right) \tag{13}$$

Substitution of A, b and c in (11) and (12) gives:

$$T_1 \left(1 + e^{\frac{-\tau}{T_2}} \right) \left(2e^{\frac{-(\tau-\theta_m)}{T_1}} - e^{\frac{-\tau}{T_1}} - 1 \right) - T_2 \left(1 + e^{\frac{-\tau}{T_1}} \right) \times \left(2e^{\frac{-(\tau-\theta_m)}{T_2}} - e^{\frac{-\tau}{T_2}} - 1 \right) = 0 \tag{14}$$

$$A_p = kh \left(2 \left(1 + e^{\frac{-\tau}{T_1}} \right)^{\frac{-T_1}{(T_1-T_2)}} \left(1 + e^{\frac{-\tau}{T_2}} \right)^{\frac{T_2}{(T_1-T_2)}} - 1 \right) \tag{15}$$

Equations (13) to (15) are solved simultaneously to estimate θ_m , T_1 and T_2 from the measurements of τ , A_p and t_p . The steady state gain k is assumed to be known a priori or can be estimated from a step signal test.

IV. Design of the controller:

G_c is considered in the following PID controller form:

$$G_c = K_c \left(1 + \frac{1}{T_i s} + \frac{T_d s}{\varepsilon T_d s + 1} \right) \tag{16}$$

Where the derivative filter constant $\varepsilon=0.1$ is typically fixed by the manufacture [15] throughout the paper. In the proposed control structure shown in Fig. 1, the nominal complementary sensitivity function for load disturbance rejection can be obtained as

$$T = \frac{GG_c}{1+GG_c}$$

(17)

In order to reject a step change in load of power system, the asymptotic constraint:

$$\lim_{s \rightarrow -\frac{1}{T_1}, -\frac{1}{T_2}} (1 - T) = 0$$

(18)

should be satisfied so that the closed-loop internal stability can be achieved. The desired closed-loop complementary sensitivity function is proposed as:

$$T = \frac{(\alpha_2 s^2 + \alpha_1 s + 1)}{(\lambda s + 1)^4} e^{-\theta_m s}$$

(19)

where λ is a tuning parameter for obtaining the desirable performance of the power system. α_1 and α_2 can be obtained from (18) and (19) $\alpha_1 = \left(T_1^2 \left((1 - \lambda/T_1)^4 e^{-\theta_m/T_1} - 1 \right) - T_2^2 \left((1 - \lambda/T_2)^4 e^{-\theta_m/T_2} - 1 \right) \right) / (T_2 - T_1)$ and $\alpha_2 = T_2^2 \left((1 - \lambda/T_2)^4 e^{-\theta_m/T_2} - 1 \right) + T_2 \alpha_1$ Using (17) and (19), we get:

$$G_c = \frac{(T_1 s + 1)(T_2 s + 1)(\alpha_2 s^2 + \alpha_1 s + 1)}{k[(\lambda s + 1)^4 - e^{-\theta_m s}(\alpha_2 s^2 + \alpha_1 s + 1)]}$$

(20)

The resulting controller G_c does not have a standard PID controller form. Therefore, in order to produce the desired disturbance rejection controller, the following procedure is employed. G_c can be approximated by an approximation series in a complex plane, by expanding it near vicinity of zero. Laurent series has been used for approximation instead of Taylor or MacLaurin series (where terms with s^0 , s^1 , and s^2 appear), Laurent series has been chosen (because the controller is given by (16), where terms with s^0 , s^{-1} , and s^1 appear, the series no longer belongs to the Taylor or Maclaurin type, but becomes Laurent type, with other coefficients as zeros) because it addresses complex coefficients that are important especially to investigate the behavior of functions near singularity. A practical desired disturbance rejection controller should possess an integral characteristic to eliminate any system output deviation arising from load disturbances. Therefore, let

$$G_c = \frac{f(s)}{s} \tag{21}$$

or

$$G_c = \frac{\gamma(s)}{s(1+\beta s)}$$

(22)

Now, expanding G_c in the vicinity of zero by Laurent series

$$G_c = \frac{1}{s(1+\beta s)} \left(\dots + \gamma(0) + \gamma'(0)s + \frac{\gamma''(0)s^2}{2!} + \dots \right)$$

(23)

The parameters of G_c obtained from (16) and (23)

$$K_c = \gamma'(0)$$

(24)

$$\frac{K_c}{T_i} = \pi r^2$$

(25)

$$K_c T_d = \frac{\gamma''(0)}{2!}$$

(26)

Thus, K_c , T_i and T_d can be obtained from equations (24) to (26).

V. Multi area power system:

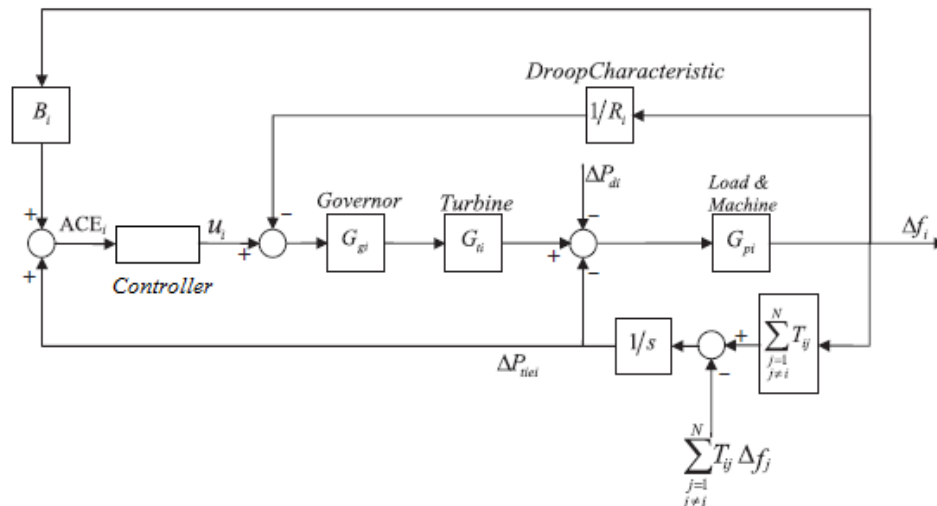


Fig.3. Linear model of control area i.

A multi area power system consists of number of single areas connected by tie-lines. If there is mismatch in frequency measure in one control area then it is not a problem of that control area power mismatch but it is the problem of all control area [20]. In decentralized power system, when load demand varies there is mismatch in frequency and tie-line power. The objective of decentralized LFC are to minimize the transient deviations of these variations maintain the steady state error to zero. For LFC control design of robust controller is a challenging task against unexpected external disturbances, parameter uncertainties and the model uncertainties. Consider multi area power system consist of N control area as shown in fig.3, in which total tie-line power change between area 1 and other area is:

$$\Delta P_{tiei} = \sum_{\substack{j=1 \\ j \neq i}}^N \Delta P_{tieij} = \frac{1}{s} \left[\sum_{\substack{j=1 \\ j \neq i}}^N T_{ij} \Delta f_i - \sum_{\substack{j=1 \\ j \neq i}}^N T_{ij} \Delta f_j \right]$$

The area control error (ACE) gives the information about frequency and tie-line power deviations, which is in turn utilized in the control strategy as shown in fig.3. The ACE for i'th control area is given as:

$$ACE_i = B_i \Delta f_i + \Delta P_{tiei} \tag{27}$$

Where B_i is the frequency bias coefficient. in multi area power system each control area should control the value of ACE to zero so as frequency and tie-line power deviations get controlled. The plant model for multi area power system is given by

$$G_i = B_i \left[\frac{G_{gi} G_{ti} G_{pi}}{1 + \frac{G_{gi} G_{ti} G_{pi}}{R_i}} \right]$$

(28)

The tuning procedure of multi area LFC is same as that of single area LFC.

VI. Simulation Results:

6.1 Simulation results for single area power system:

Consider a power system with a non-reheated turbine and a reheated turbine. The model parameters are Non-reheated turbine: $K_p= 120, T_p= 20, T_T=0.3, T_G= 0.08, R= 2.4$.

Reheated turbine: $K_p= 120, T_p= 20, T_T= 0.3, T_G= 0.08, R= 2.4, T_r= 4.2$ and $c=0.35$.

By selecting suitable value of λ and β , the controller settings (see Table 1) for the power system with non-reheated and reheated turbines can be obtained using equations (24) to (26). By the help of extensive simulation study, $\lambda = 0.13$ and $\beta = 0.012$ for NRTWD, $\lambda = 0.11$ and $\beta = 1$ for NRTD, $\lambda = 0.05$ and $\beta = 0.0035$ for RTWD and $\lambda = 0.1$ and $\beta = 3$ for RTD. Figs. 4 and 5 show the frequency changes of the power system following a load demand $\Delta P_d = 0.01$. The stability robustness is tested by changing the parameters (K_p, T_p, T_T, T_G) of the system by $\pm 50\%$. From the simulation results, it is evident that the proposed method gives better performance.

Table 1. Identified model and controller parameters.

Plant	Identified model	Controller parameters
NRTWD	$\frac{120e^{-0.4626s}}{(28.4952s + 1)(0.2202s + 1)}$	$K_c = 1.0326, T_i = 1.2116, T_d = 0.3420$
NRTD	$\frac{250e^{-0.05s}}{(2.028s^2 + 12.765s + 106.2)}$	$K_c = 1.4978, T_i = 1.1481, T_d = 0.1574$
RTWD	$\frac{120e^{-0.541s}}{(23.2137s + 1)(0.9057s + 1)}$	$K_c = 3.6317, T_i = 1.0998, T_d = 0.4828$
RTD	$\frac{235.3e^{-0.035s}}{(1.79s^2 + 16.9s + 100)}$	$K_c = 6.164, T_i = 3.1934, T_d = 0.1882$

NRTWD: non-reheat turbine without droop; NRTD: non-reheat turbine with droop; RTWD: reheat turbine without droop; RTD: reheat turbine with droop.

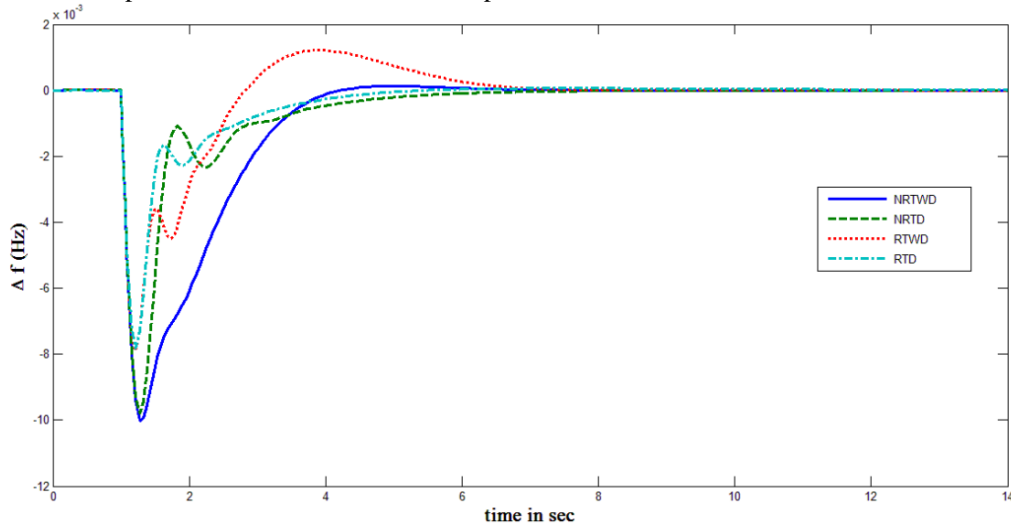


Fig.4. Frequency deviations for single area power system with nominal parameters.

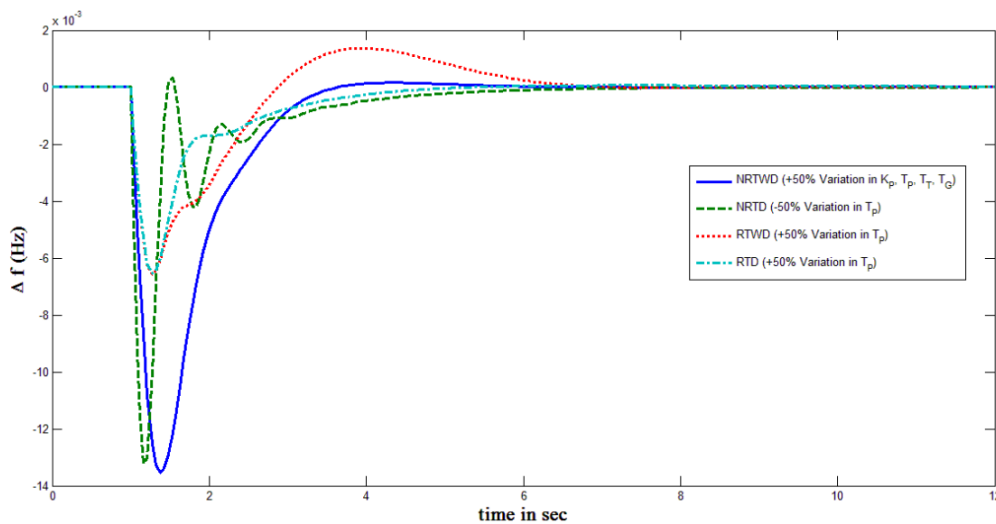


Fig.5. Frequency deviations for single area power system with parameter variations.

6.2 Simulation results for multi area power system:

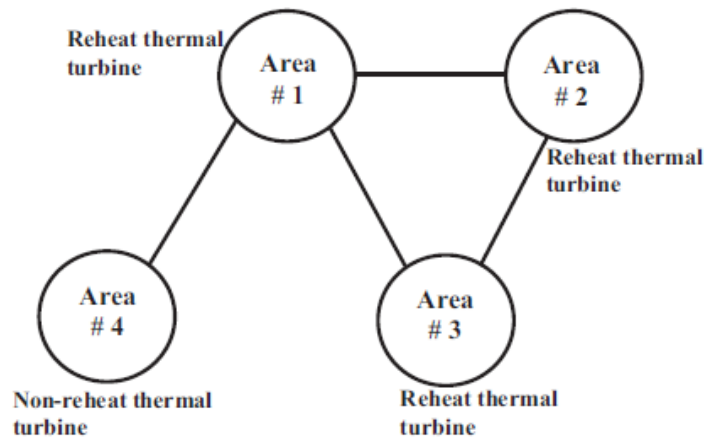


Fig.6. Simplified diagram of a four area power systems.

The simplified diagram of a four area power systems is shown in Fig.6. In the simulation results, area 1, area 2 and area 3 are denoted as the area with reheat unit, and area 4 is denoted as the area with non-reheat unit. The parameters of the non-reheat and reheat units in different areas are chosen as, Nominal parameters for area 1, area 2 and area 3: $T_{P1} = T_{P2} = T_{P3} = 20$, $T_{T1} = T_{T2} = T_{T3} = 0.3$, $T_{G1} = T_{G2} = T_{G3} = 0.2$, $K_{P1} = K_{P2} = K_{P3} = 120$, $R_1 = R_2 = R_3 = 2.4$, $T_{r1} = T_{r2} = T_{r3} = 20$, and $c_1 = c_2 = c_3 = 0.333$. Nominal parameters for area 4: $K_{p4} = 120$, $T_{p4} = 20$, $T_{T4} = 0.3$, $T_{G4} = 0.08$, $R_4 = 2.4$.

The synchronizing constants are $T_{12} = T_{23} = T_{31} = T_{41} = 0.0707$ and the frequency bias constants are $B_1 = B_2 = B_3 = B_4 = 0.425$. The identified model of plant for reheat unit with droop characteristic is obtain as $G = 0.9965e^{-0.5s}/(0.72s^2+1.7s+1)$ and that for non-reheat unit with droop is same as that of given in Table 1. By choosing $\lambda = 0.7$ and $\beta = 0.35$, the controller settings for area 1, area 2 and area 3 are $K_c = 1.1895$, $T_i = 1.9090$ and $T_d = 0.5454$. Similarly, the controller parameters for area 4 are $K_c = 1.9822$, $T_i = 0.5242$ and $T_d = 0.1756$ by taking $\lambda = 0.1$ and $\beta = 0.35$.

To show the performance of the decentralized sliding mode controller, a step load $\Delta P_{d1} = 0.01$ is applied to area 1 at $t = 5$ s, followed by a step load $\Delta P_{d3} = 0.01$ to area 3 at $t = 100$ s. Fig. (7 to10) illustrates the frequency errors of the four different areas. Fig. (11 to 14) shows the tie-line power errors of the four areas. From the simulation results, it can be seen that the frequency errors, and tie-line power deviations have been driven to zero by proposed controller in the presences of power load changes.

In order to test the robustness of the controller, the variations of the parameters of the non-reheat and reheat units in the four areas are assumed to be $\pm 50\%$ of their nominal values. However, the controller parameters are not changed with the variations of the system parameters. Fig. (7 to 10) illustrates the frequency errors of four areas with the variant parameter values. Fig. (11 to 14) shows the tie-line power errors of the four areas with the variant parameter values. From the simulation results, it can be seen that despite such large parameter variations, the system responses do not show noticeable differences from the nominal values. Therefore, the simulation results demonstrate the robustness of proposed controller against system parameter variations. It is observed that the proposed decentralized PID controller achieves better damping for frequency and tie-line power flow deviations in all the four areas.

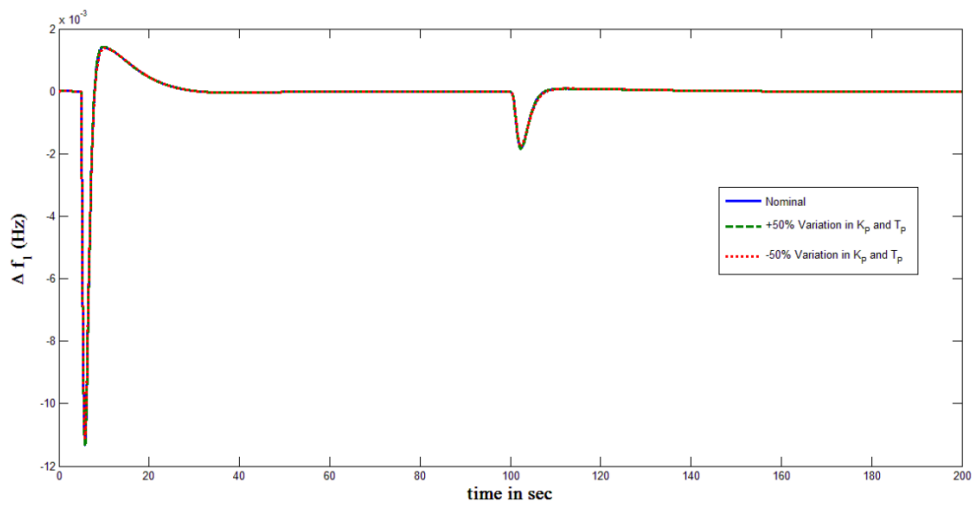


Fig.7. Frequency deviation of area 1 of four area power systems.

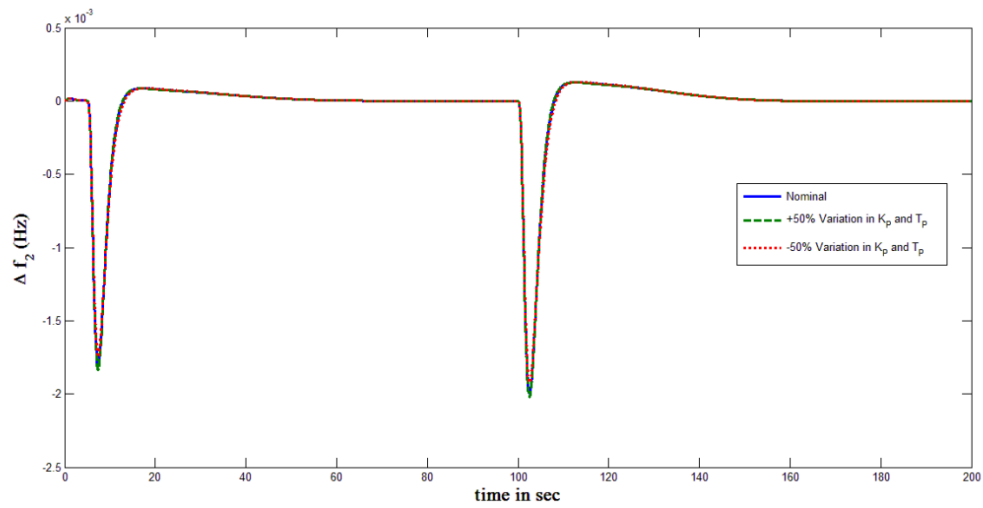


Fig.8. Frequency deviation of area 2 of four area power systems.

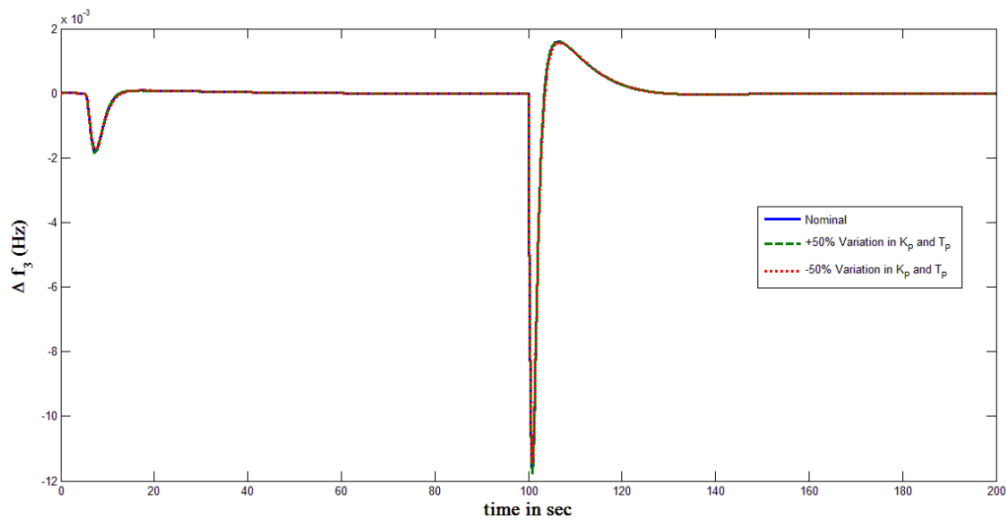


Fig.9. Frequency deviation of area 3 of four area power systems.

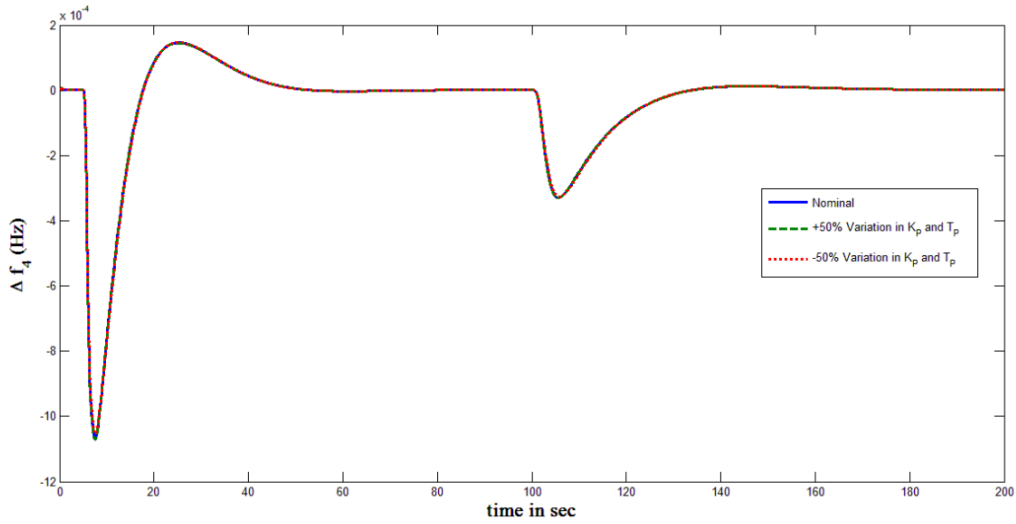


Fig.10. Frequency deviation of area 4 of four area power systems.

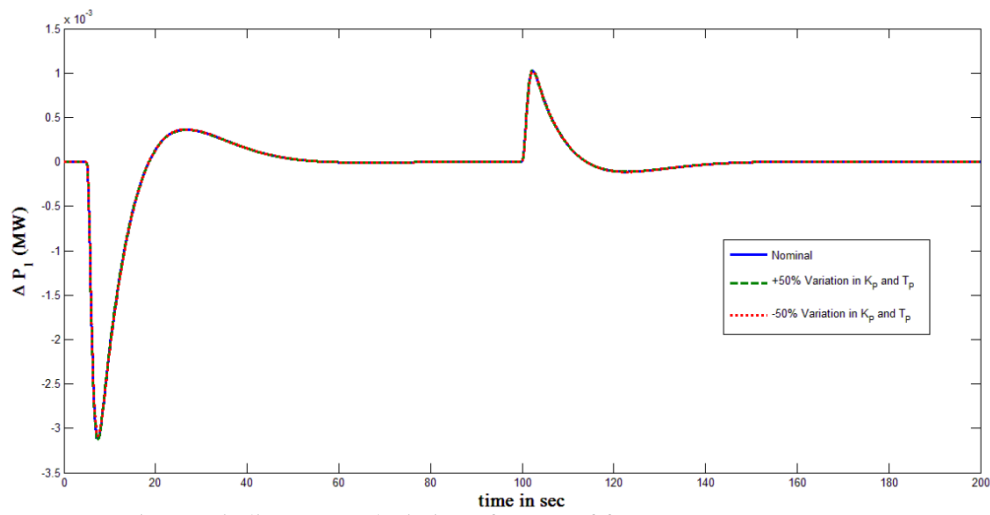


Fig.11. Tie line power deviation of area 1 of four area power systems.

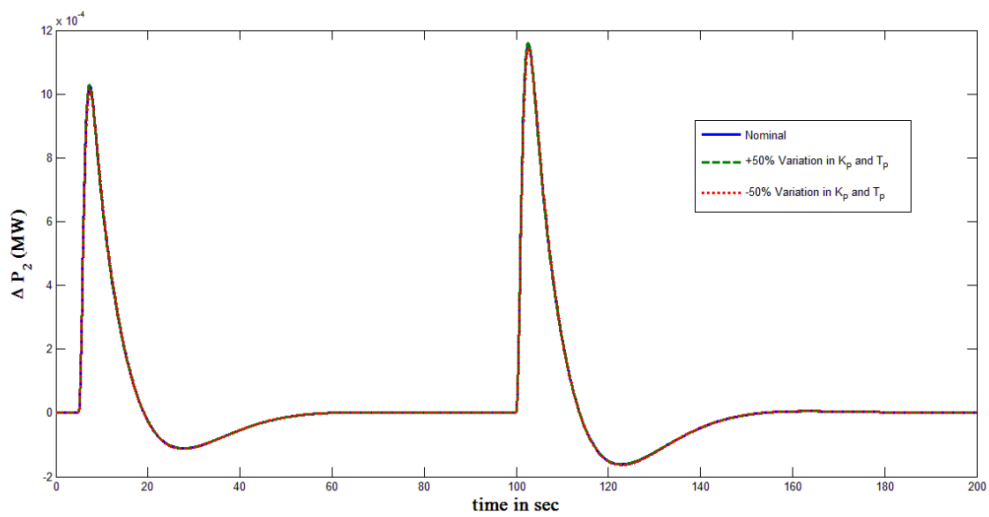


Fig.12. Tie line power deviation of area 2 of four area power systems.

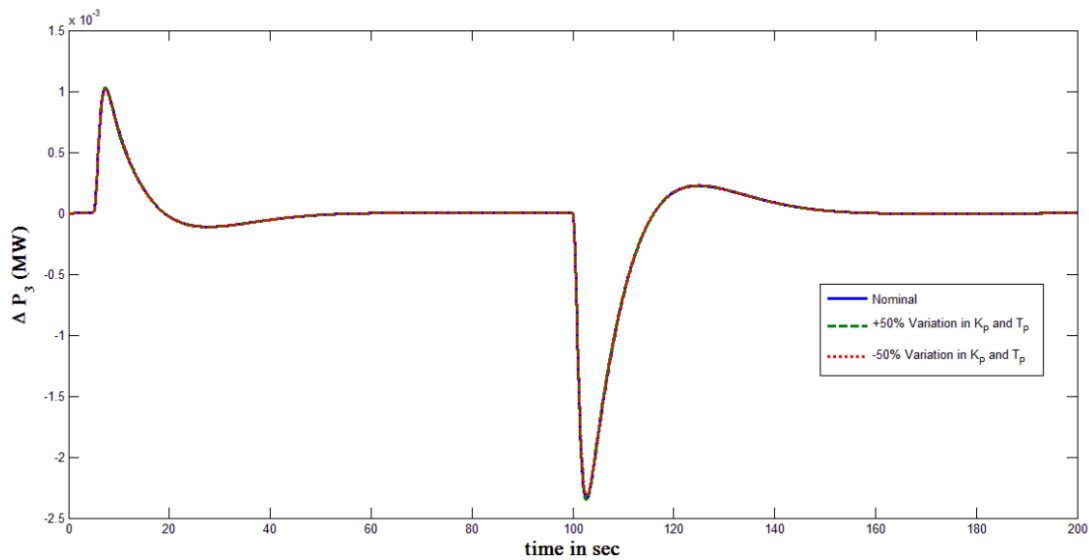


Fig.13. Tie line power deviation of area 3 of four area power systems.

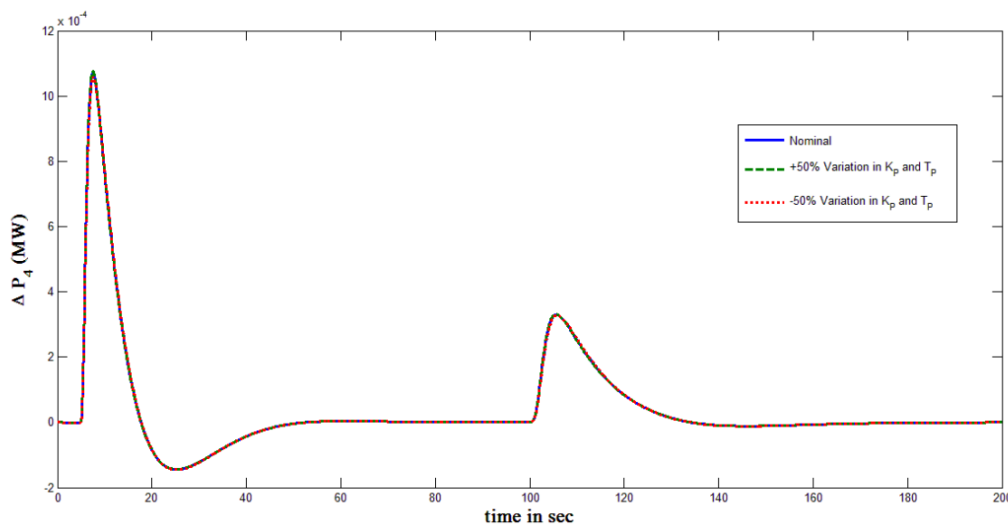


Fig.14. Tie line power deviation of area 4 of four area power systems.

VII. Conclusion:

The LFC characteristics of a single-area power system with non- reheat and reheat turbines have been studied. A relay feedback test has been conducted to estimate the parameters of the power system. The results show that the proposed PID controller with a new structure gives a better performance in load disturbance rejection and robustness. The proposed method is applied to a four-control area power system and tested with different plant parameters uncertainty scenarios.

References:

- [1] Kundur P. Power system stability and control. New York: McGraw-Hill; 1994.
- [2] Jaleeli N, VanSlyck LS, Ewart DN, Fink LH, Hoffmann AG. Understanding automatic generation control. IEEE Transactions on Power Systems 1992;7(August (3)):1106–22.
- [3] Ibraheem, Kumar P, Kothari DP. Recent philosophies of automatic generation control strategies in power systems. IEEE Transactions on Power Systems 2005;20(1):346–57.
- [4] Tomsovic K, Bakken DE, Venkatasubramanian V, Bose A. Designing the next generation of real-time control, communication, and computations for large power systems. Proceedings of the IEEE 2005;93(5):965–79.
- [5] Kothari M, Sinha N, Rafi M. Automatic generation control of an interconnected power system under deregulated environment. Power Quality 1998;18: 95–102.
- [6] Donde V, Pai MA, Hiskens IA. Simulation and optimization in an AGC system after deregulation. IEEE Transactions on Power Systems 2001;16:481–9.
- [7] Okada K, Yokoyama R, Shirai G, Sasaki H. Decentralized load frequency control with load demand prediction in multi-area power systems. Proceedings of International Conference on Control 1988;13(15):649–54.
- [8] Aldeen M, Sharma R. Robust detection of faults in frequency control loops. IEEE Transactions on Power Systems 2007;22(1):413–22.

- [9] Bevrani H, Hiyama T. Robust decentralized PI based LFC design for time delay power systems. *Energy Conversion and Management* 2008;49(2):193–204.
- [10] Moon Y, Ryu H, Lee J, Kim S. Power system load frequency control using noise-tolerable PID feedback. *IEEE International Symposium on Industrial Electronics* 2001;3:1714–8.
- [11] RerkPreedapong D, Hasanovic A, Feliachi A. Robust load frequency control using genetic algorithms and linear matrix inequalities. *IEEE Transactions on Power Systems* 2003;18(2):855–61.
- [12] Yu X, Tomsovic K. Application of linear matrix inequalities for load frequency control with communication delays. *IEEE Transactions on Power Systems* 2004;19(3):1508–15.
- [13] Tan W. Unified tuning of PID load frequency controller for power systems via IMC. *IEEE Transactions on Power Systems* 2010;25(1):341–50.
- [14] Khodabakhshian A, Edrisi M. A new robust PID load frequency controller. *Control Engineering Practice* 2008;16:1069–80.
- [15] O'Dwyer A. *Handbook of PI and PID controller tuning rules*. 2nd edition Imperial College Press; 2006.
- [16] Balaguer P, Alfaro V, Arrieta O. Second order inverse response process identification from transient step response. *ISA Transactions* 2011;50(2): 231–8.
- [17] Mei H, Li S. Decentralized identification for multivariable integrating processes with time delays from closed-loop step tests. *ISA Transactions* 2007;46(2):189–98.
- [18] Natarajan K, Gilbert A, Patel B, Siddha R. Frequency response adaptation of pi controllers based on recursive least-squares process identification. *ISA Transactions* 2006;45(4):517–28.
- [19] Majhi S. Relay based identification of processes with time delay. *Journal of Process Control* 2007;17:93–101.
- [20] Bevrani H. *Robust power system frequency control*. Springer; 2009.